ADVANCED MATERIALS TECHNOLOGIES
www.advmattechnol.de

Variable Stiffness Actuators with Covalently Attached Nanofragments that Induce Mineralization

*Danfeng Cao, Jose G. Martinez, Emilio Satoshi Hara, and Edwin W. H. Jager**

Soft robotics has attracted great attention owing to their immense potential especially in human–robot interfaces. However, the compliant property of soft robotics alone, without stiff elements, restricts their applications under load-bearing conditions. Here, biohybrid soft actuators, that create their own bone-like rigid layer and thus alter their stiffness from soft to hard, are designed. Fabrication of the actuators is based on polydimethylsiloxane (PDMS) with an Au film to make a soft substrate onto which polypyrrole (PPy) doped with poly(4-styrenesulfonic-co-maleic acid) sodium salt (PSA) is electropolymerized. The PDMS/Au/PPy(PSA) actuator is then functionalized, chemically and physically, with plasma membrane nanofragments (PMNFs) that induce bone formation within 3 days, without using cells. The resulting stiffness change decreased the actuator displacement; yet a thin stiff layer couldnot completely stop the actuator's movement, while a relatively thick segment could, but resulted in partial delamination the actuator. To overcome the delamination, an additional rough Au layer was electroplated to improve the adhesion of the PPy onto the substrate. Finally, an alginate gel functionalized with PMNFs was used to create a thicker mineral layer mimicking the collagen-apatite bone structure, which completely suppressed the actuator movement without causing any structural damage.

1. Introduction

Soft robotics has gained great attention in the last decades with an increasing demand in broad applications, including in healthcare, such as in medical devices for surgery,[1] augmentation of human movement during rehabilitation as assistive devices,[2] mimicking the human body for advanced prostheses,[3] and biosensing.[4]

However, although soft robots predominantly use soft materials to achieve compliance or to enable a safe interaction with humans, stiff segments or stiff components are still essential as load-bearing structures. For instance, Calisti et al. designed an ad hoc robot using stainless steel as a load bearing to assist in crawling forward.[5] Naficy et al. developed a poly(*N*-isopropylacrylamide) -based temperature-sensitive polymer network, combined with the polymer poly(2-hydrox-yethyl methacrylate), to provide structural integrity and connect the bending parts of the actuator as hinges to achieve movement and shape control.[6] Xu et al. incorporated hard 2D layered materials as an endoskeleton in a 3D soft robotic to support its body.[7]

Such stiff segments can be integrated directly during fabrication by using materials with different mechanical properties or made by using materials that undergo physical–chemical changes by external stimuli, such as light, temperature, and magnetic fields, so-called 4D printing. Examples of the former method are for instance: Tyagi et al. fabricated patterned polydimethylsiloxane (PDMS) having parts of different thicknesses of PDMS obtaining both soft and stiff segments.[8] Xu et al. added Zn^{2+}-imidazole cross-links to enhance the stiffness of the elastomer.[9] Gharazi et al. presented a hybrid hydrogel with different stiffness zones, using silica nanoparticles to increase the cross-linking.[10] Alici et al. used carbon fibers as a rigid body and hardened them with resin to move the device in a direction perpendicular to the longitudinal axis of the device body. The device can be considered like a fish having pectoral fins with a carapace (rigid body) with side or paired fins running through the rigid body.[11] Smela et al. also integrated rigid elements with flexible, soft segments, as hinges for controlled folding of the predetermined shape of a microstructure.[12]

On the other hand, to make these stiff segments, one can use materials that can change mechanical properties, from soft to rigid, when they undergo external stimulation, that is, variable stiffness such as shape memory polymers (SMP), shape memory alloys (SMA), low melting point alloys (LMPA), and magnetorheological fluid (MRF). Yang et al. developed a variable stiffness actuator introducing a stiffness variable polyolefin

D. Cao, J. G. Martinez, E. W. H. Jager
Sensor and Actuator Systems
Department of Physics, Chemistry and Biology (IFM)
Linköping University
Linköping 58183, Sweden
E-mail: edwin.jager@liu.se
E. S. Hara
Department of Biomaterials
Graduate School of Medicine
Dentistry and Pharmaceutical Sciences
Okayama University
Okayama 700-8558, Japan
The ORCID identification number(s) for the author(s) of this article can be found under https://doi.org/10.1002/admt.202201651.

DOI: 10.1002/admt.202201651

elastomer (an SMP) and a phase change material, that is, paraffin wax. This tuneable reversible deformation and mechanical transformation actuator had a high load-bearing capability.[13] Yang et al. designed a microtentacle soft actuator based on SMA that could transform to a fixed and stiff bending shape when the temperature cooled, demonstrating the performance by gripping and manipulating small-scale objects.[14] Tonazzini et al. proposed a variable stiffness fiber by embedding LMPA into silicone rubber tubing to achieve reversible stiff-to-soft switching.[15] Jiang et al. presented an MRF-Robot, which could freely and rapidly transform between stiff and soft states under the actuation of magnetic fields.[16]

Inspired by the initial steps of bone tissue development, similar to how the fontanelle bone of a mammalian embryonic skull transforms from a soft and flexible tissue to a rigid tissue, we have recently developed biohybrid soft-to-hard actuators that self-create bone.[17] The soft-to-hard actuators consisted of alginate (Alg) hydrogels functionalized with cell-derived plasma membrane nanofragments (PMNFs), which were shown to induce fast mineralization within only 2 days[18,19] and polypyrrole (PPy) as the electromechanically active layer. Incubation in minimum essential medium (MEM) induced mineralization of the PMNFs in the hydrogel layer, turning the actuator rigid, and thereby completely stopping its movement.[17] The designed actuator is a demonstration of variable stiffness change based on self-induced bone growth, more specifically through PMNF-initiated mineralization, and could even have its applications expanded to more sophisticated devices, for example, linear polymeric actuators or complex soft robots. For example, soft robotics could be designed to be initially soft and free to deform, and then be easily inserted through small orifices, such as a needle or catheter. After insertion, they can unfold or deploy and be induced to become hard in total or in part and attain load-bearing properties, for instance, in the repair of complicated or inaccessible surgical sites in the spine. In all these cases, it is convenient to have hard or fixed parts of the robots/devices, which are not subjected to a fully reversible actuation. Moreover, an advantage of the PMNF-based biohybrid material is that this phase change is achieved in mild conditions, that is, at room temperature in a Ca^{2+} and phosphate-containing solution, instead of using potentially harmful conditions, such as elevated temperatures, high voltage, or UV light, especially for applications in tissue engineering.

As mentioned, in these soft-to-hard actuators, PPy is used as the electromechanically active component. Conducting polymers (CPs), such as PPy, are materials that can be reversibly electrochemically oxidized and reduced in an electrolyte resulting in a change in their properties such as conductivity and volume. When macro-ions (e.g., polycarboxylic acid, COO^-) are used as counterions in PPy, during reduction electrons are injected into the polymer chains, and cations (and water molecules) enter into the PPy matrix to compensate for the negative charge of COO^-, causing the PPy film to swell. During oxidation, electrons are ejected from the polymeric chains and positive charges are stored along the chains that now compensate for the negative charges of COO^-, and cations are expelled from PPy into the solution to maintain electrical neutrality, leading the PPy film to shrink. Conducting polymers with the capability of reversible dimensional changes can be used as the active layer to construct various electrochemical actuators in combination with other passive layers, such as a thin Au layer, to achieve bending actuation.[20] The contraction/expansion motion of the electroactive CP layer creates the driving force to bend the actuator.

In our previous soft-to-hard actuators, the PMNFs were immobilized using so-called physical immobilization, that is, entrapment in the hydrogel combined with electrostatic attraction with the crosslinking-Ca^{2+} ions. Since chemical immobilization is more stable than physical, and in order to expand the application areas of the PMNF-induced bone formation, we devised a chemical immobilization procedure to directly and covalently bind the PMNFs on the PPy surface using 1-ethyl-3-(3-dimethylaminopropyl) carbodiimide hydrochloride/*N*-hydroxysuccinimide (EDC/NHS) coupling.[21] Therefore, this study aimed to investigate the effect of covalently bound PMNFs and the formation of the minerals on the actuator's mechanical properties during the soft-to-hard phase change of the actuators.

2. Results and Discussion

2.1. Fabrication and Optimization of PDMS/Au/PPy Actuators

A flexible substrate with a conductive (metal) layer is an important prerequisite for the fabrication of durable, soft, electrochemical actuators. PDMS is a widely used soft material in flexible electronics and biomedical devices because of its biocompatibility, excellent flexibility, and elastic properties.[22] However, PDMS is an insulating material that hinders the possibility to directly electropolymerize PPy on its surface to fabricate a soft actuator with an active bending layer of PPy and a passive layer of PDMS. Thus, an intermediate electrically conductive layer is necessary.[8,23] However, the fabrication of an Au layer onto the PDMS layer is challenging.

Conventional techniques for direct metal deposition on PDMS, such as thermal evaporation, usually need high temperature and vacuum, leading to cracking of the metal layer due to the large mismatch in the coefficients of thermal expansion of PDMS and metals, as well as to structural damage of the PDMS layer due to its low melting point.[24] To overcome this issue, a metal layer can be prepared on rigid substrates, such as a Si wafer, and subsequently be transferred onto PDMS.[25] Here, we developed an easy and low-cost method to prepare the PDMS/Au passive substrate by transferring the Au metal layer from the Au/Si wafer to PDMS, as illustrated in **Figure 1**. **Figure 2**a shows the PDMS/Au passive substrate with an intact coating of Au film on the surface of PDMS and excellent flexibility without any breakage (Figure 2b). Further tape-testing of the Au film on the PDMS (Figure 2c,d) did not show any significant destruction of the Au coating on the PDMS layer. The conductivity of the PDMS/Au passive substrate was still high after the tape testing experiment (9.78×10^6 S m^{-1} before and 3.98×10^6 S m^{-1} after tape testing) (Table S1, Supporting Information). The scanning electron microscopy (SEM) image in Figure 2e shows disordered wrinkles of the Au layer with an average period of 6–8 μm. This wrinkling of the surface can be attributed to the shrinkage of PDMS during the curing.

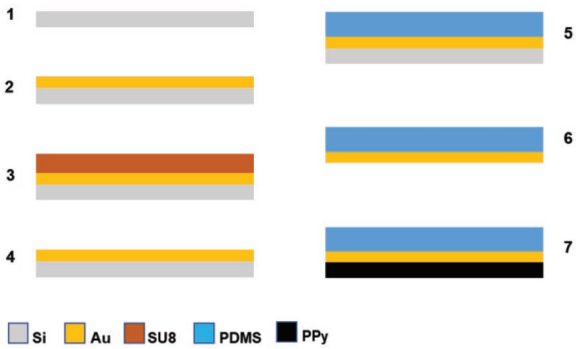

Figure 1. Fabrication procedures of PDMS/Au passive substrate and PDMS/Au/PPy actuator. 1) Si wafer, 2) Evaporate Au on Si wafer, 3) Spin-coat SU 8 on the Au surface, 4) SU 8 development and stripping from the Au surface, 5) Spin-coat PDMS on the gold surface, 6) Peel off the PDMS with Au film from the Si wafer, and 7) electropolymerize PPy on the PDMS/Au substrate.

The flexible PDMS/Au passive substrate was then used as the substrate for PPy electropolymerization to make the PDMS/Au/PPy actuator. PPy was synthesized using three different synthesis charges, 1, 2, and 3 C. Figure 2f shows the PDMS/Au substrate with the electropolymerized PPy doped with poly (4-styrenesulfonic acid-co-maleic acid) sodium salt (PSA) prepared by consuming 1 C charge. It formed a compact and uniform black layer on the PDMS/Au. The good flexibility was retained after the deposition of the PPy actuation layer under folding (Figure 2g). The morphology of PPy films also showed the same wrinkled structure (Figure 2h). As expected, the electropolymerization of PPy using different synthesis charges (1, 2, and 3 C) resulted in increased thickness of PPy film from 2.3 µm for PPy(PSA)1C to 4.2 µm for PPy(PSA)3C (Figure S1, Supporting Information).

Figure S2, Supporting Information, shows the bending of the fabricated bilayer actuator, which followed the movement of a cation-driven actuator, that is, during reduction, the PPy layer swells by insertion of cations and water, while during oxidation, it shrinks by the expulsion of cations and water.[26] Next, the actuation behavior of the resulting PDMS/Au/PPy actuators with different PPy thicknesses was investigated. As can be seen in Figure S2, Supporting Information, the 1 and 2 C actuators have good actuation performance. They displayed typical actuation cycles with 3 and 4 mm displacement, respectively. A rapid displacement within less than 1 s can be observed during the switching of reduction/oxidation, which is fast for such electrochemomechanical actuators with relatively thick PPy layers, based on the volume changes caused by the insertion/expulsion of ions and water.[27,28] Each cycle of the actuator was actuated for 200 s to illustrate that the actuator is stable at maximum displacement (Figure S3, Supporting Information). For comparison, the two actuators showed much faster-bending movement than our previously developed PPy/Alg gel actuators.[17] On the other hand, the 3 C actuator showed a rapid movement of 1 mm at the beginning of the reduction cycle, with no obvious actuation thereafter. In addition, the PPy film was showing cracks and delamination at the beginning of the actuation caused by the high stiffness with the increased synthesis charge, that is, the thicker PPy layer. Hence, the 3 C actuator was not used in subsequent studies. Next, only the 1 and 2 C actuators were incubated in MEM for 3 days. The actuation behavior of 1 and 2 C actuators after MEM incubation is shown in Figure S4, Supporting Information. Only the 1 C actuator showed complete and intact adherent PPy film on the PDMS/Au passive substrate both before and after actuation, while in the case of the 2 C actuator, a few cracks and swelling-induced delamination appeared on the actuator's surface after several actuation cycles between −0.7 and +0.5 V indicating a start of the delamination between PPy and PDMS/Au (Figure S5, Supporting Information). Therefore, only the 1 C actuator was used for further studies.

2.2. The Effect of PMNF-Induced Mineralization on the Actuators

As mentioned, PMNFs can promote rapid mineralization in vitro through the formation of amorphous calcium phosphate

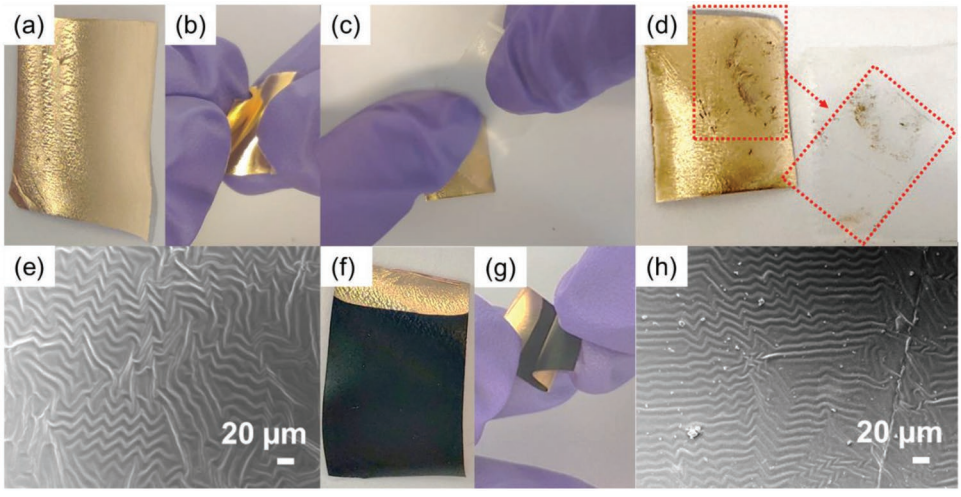

Figure 2. a) Digital image of PDMS/Au device and b) its folding; digital image c) during and d) after PDMS/Au tape-tearing; e) top-view of SEM image of PDMS/Au passive substrate; f) digital image of 1 C actuator and g) its folding; h) top-view of SEM image of 1 C actuator.

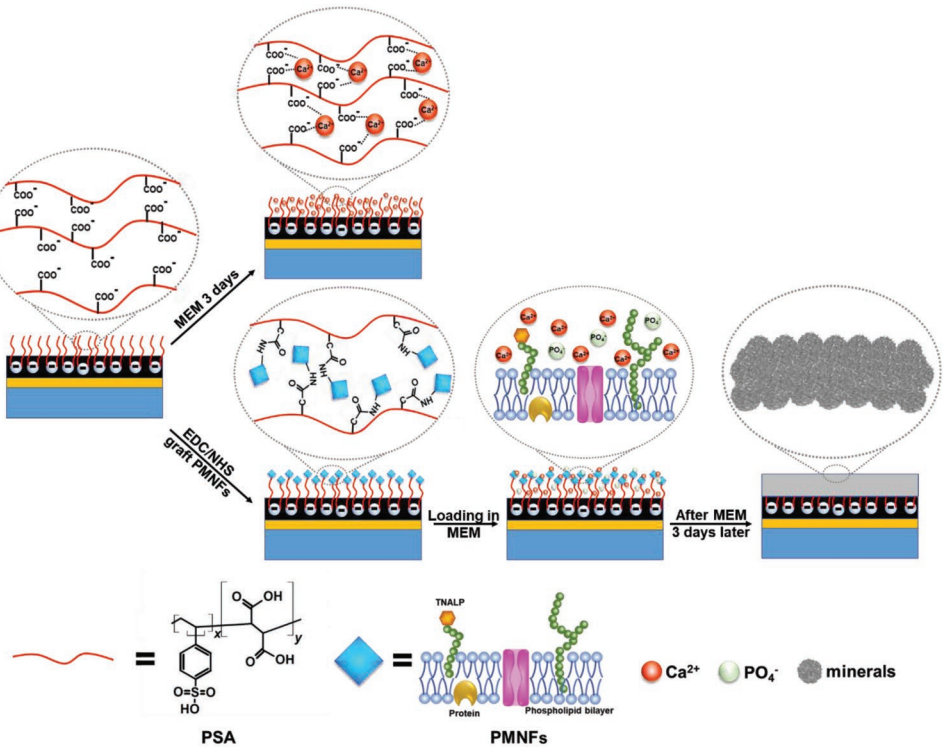

Figure 3. Schematic diagram of the layers of the PPy actuator without and with PMNFs. The PMNFs when incubated in MEM induce mineral formation onto the PPy layer.

(ACP) in the initial 3 days of MEM incubation; with a subsequent transformation of ACP into apatite crystals after 7 days of MEM incubation.[18] In our previous work, we demonstrated the application of PMNFs for the fabrication of a variable stiffness actuator based on PPy using a physical immobilization in an Alg gel.[17] In this present study, we further evaluate the effect of PMNF-induced mineralization using covalent immobilization. The PMNFs were covalently immobilized on the PPy(PSA)1C layer by EDC/NHS chemistry as shown in **Figure 3**. The actuation behavior of the actuator with PMNFs before and after MEM incubation was tested in 0.1 M NaCl with applied reduction and oxidation potentials. Typical actuation behavior, without delamination from the PDMS/Au passive substrate, can be observed for the actuator with PMNF before MEM incubation (**Figure 4**a–c), which is consistent with the actuator without PMNF before incubation (Figure S2, Supporting Information), indicating that PMNFs themselves have little effect on the actuator movement. After incubation in MEM, the bending of the actuator with PMNFs was completely blocked by the formation of the mineral layer (Figure 4b,c) during the first actuation cycle. However, at the start of the second redox cycle, the PPy layer fractured and delaminated (Figure 4b), leading to delamination of the PPy and PDMS/Au substrate layers, that is, they were no longer mechanically connected, followed by permanent damage of the actuator, which showed no further significant movement (Figure 4c). Moreover, PMNF mineralization caused a decrease in the current compared with the results before mineralization, which we attribute to a decreased conductive surface and the cracking of the PPy layer (Figure 4d). Note that the current passing through actuators after mineralization was almost zero, except for the sharp peak at the second redox cycle when rapid movement and instant delamination of the actuator film surface was seen (Figure 4d).

The surface characteristics were analyzed by SEM and revealed cracks and major delamination in the actuated actuator with PMNFs (**Figure 5**). On the other hand, the actuator with PMNFs that was not incubated in MEM remained intact even after actuation (Figure 5a).

High magnification SEM images of the actuator's surface morphology and elemental composition obtained by energy-dispersive X-ray spectroscopy (EDX) revealed a typical "cauliflower" morphology characteristic of PPy[29] in all samples before MEM incubation, as well as in the actuator without PMNFs after MEM incubation (**Figure 6**a–f). When the actuator with PMNFs was incubated in MEM, granular minerals were formed from PMNF activity,[17] and a high Ca peak was observed in the EDX spectra (Figure 6g), indicating indeed the formation of minerals on the PPy surface. However, after actuation, the amount of granular minerals apparently decreased on the actuator with PMNFs incubated in MEM, showing now a "cauliflower" surface morphology comparable to that before MEM incubation (Figure 6h). This was also confirmed by the decreased Ca peak intensity in the EDX spectra. These results could be attributed to the simultaneous burst and detachment of the minerals from the PPy surface during the cracking and delamination of PPy film from the PDMS/Au passive substrate. Note also that the Ca peak, which is absent in all samples before MEM incubation, can be detected in the 1 C actuator without PMNFs after MEM incubation likely due to the cross-linking of polycarboxylic acid chains in PSA with Ca^{2+} ions in MEM.

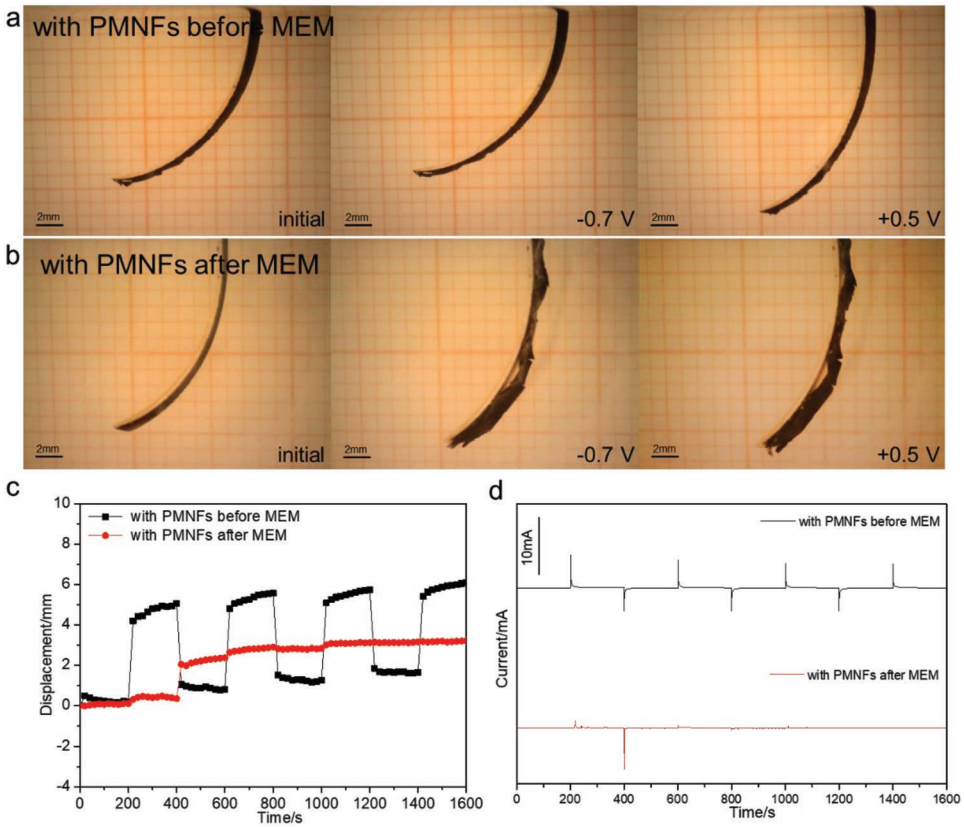

Figure 4. Actuation of PPy actuators with PMNFs a) before and b) after MEM incubation at an initial reduction (–0.7 V) and oxidation (+0.5 V) states. Corresponding c) displacement and d) current curves during actuation.

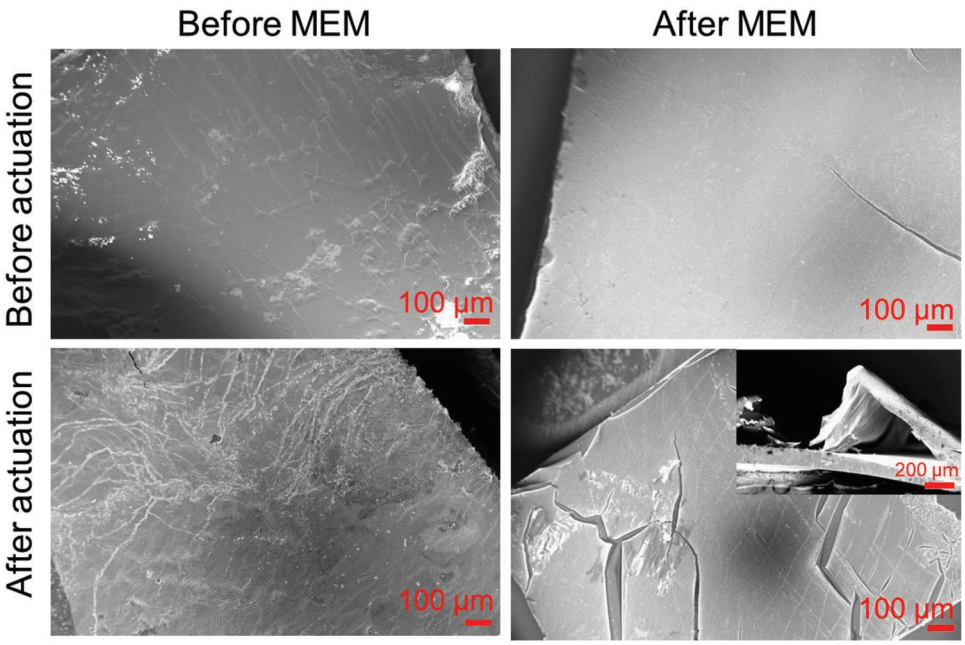

Figure 5. SEM images of actuators with PMNFs before and after MEM incubation, before and after actuation. The inset in the right lower image shows the cross-sectional view of the actuator with PMNFs after MEM incubation and after actuation showing the delamination.

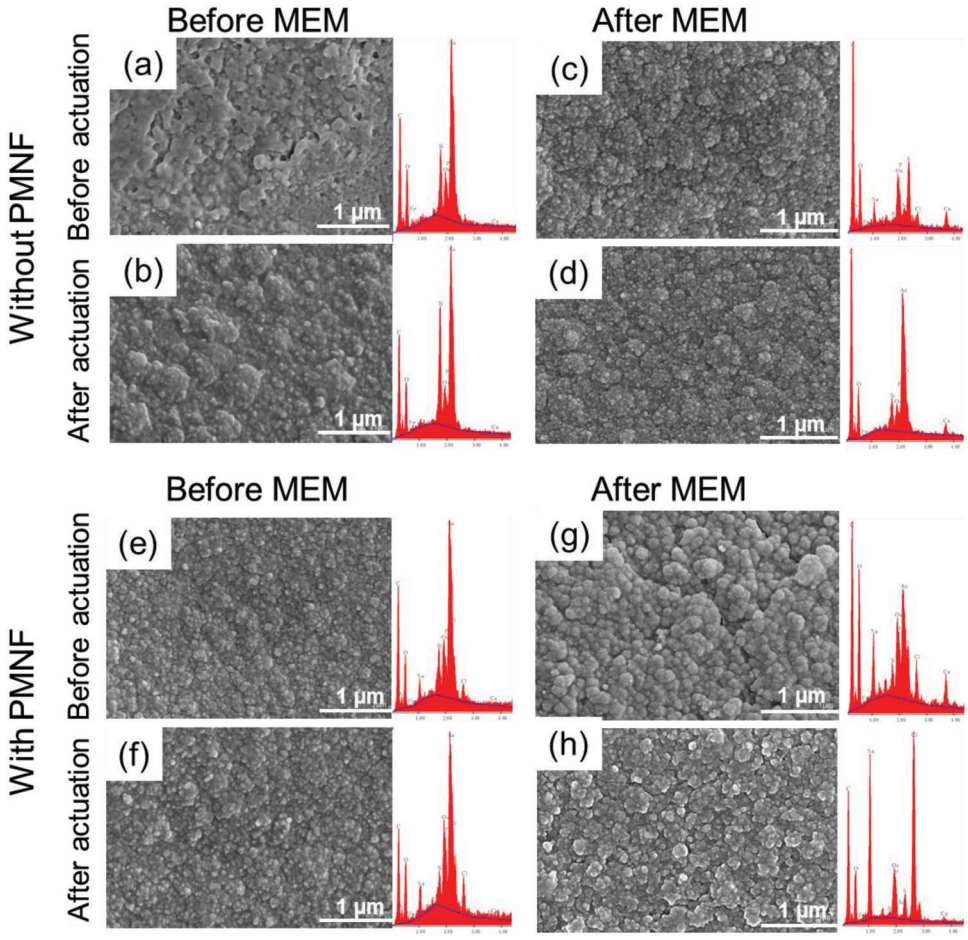

Figure 6. SEM images and EDX spectra of 1 C actuator without PMNFs a) before and c) after MEM incubation, and b) before and d) after actuation compared to those of 1 C actuator with PMNFs e) before and g) after MEM incubation and f) before and h) after actuation.

2.3. Increase in Bending Stiffness

The bending stiffness can be calculated using classical bending beam theory,[30] and several complex multilayer models have been developed.[31] However, since we are interested in the stiffness change at the device level, experimental bending stiffness measurements were performed on the full actuator by placing the tip of the lever arm transducer at the tip of the actuator and measuring the deflection at different applied forces.[32] To study the effect of PPy(PSA) thickness and mineralization on the mechanical properties, the experimental stiffness values k for different actuators before and after MEM incubation were calculated using the standard bending beam formula (1),

$$\delta = \frac{FL^3}{3EI} \tag{1}$$

where E is the equivalent Young's modulus and I the equivalent moment of inertia of the actuator, F is the force applied on the actuator tip, L is the length of the actuator from the force point to the fixed point of the clamp, and δ is the bending distance as shown in **Figure 7**a.

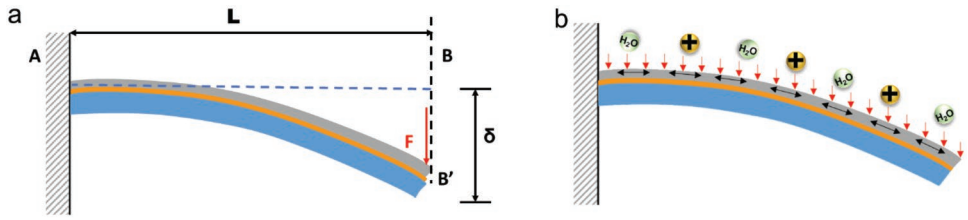

Figure 7. a) Illustration of the bending beam definitions for the actuator as used in the stiffness k calculation (Equation (3)); b) Illustration of the actuation and subsequently generated force in the PPy layer of the actuators upon electrochemical activation.

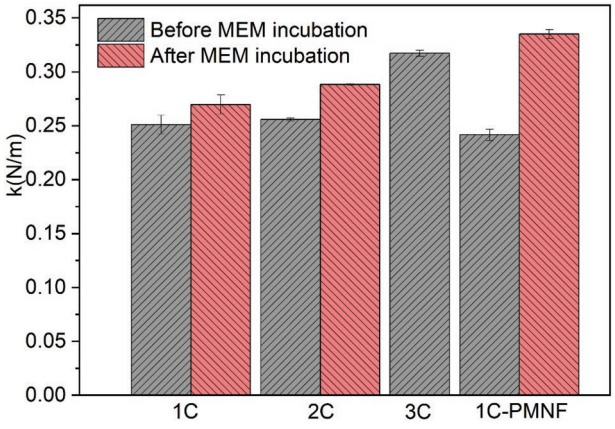

Figure 8. The bending stiffness values k for the different PPy actuators before and after MEM incubation. Note the significant increase in the k of 1 C actuator with PMNF after incubation in MEM, as a result of PMNF-induced mineralization.

This can be rewritten as

$$F = \frac{3EI}{L^3}\delta \tag{2}$$

or

$$F = k * \delta \tag{3}$$

with k the experimental bending stiffness of the actuator.

As shown in **Figure 8** and Figure S7, Supporting Information, in the actuators (before incubation in MEM), the calculated k value increased with the increase of synthesis charge (i.e., PPy thickness), which were 0.25, 0.26, and 0.32 N m^{-1} for 1, 2, and 3 C actuators, respectively. The 1 C and 2 C actuators also showed a small increase in the k value to 0.27 and 0.29 N m^{-1}, respectively, after MEM incubation (Figure 8). We contribute this to the cross-linking of polycarboxylic acid chains in PSA with Ca^{2+} ions during the incubation forming a PSA-"layer" which increases the stiffness. Analysis of 3 C was not possible due to the crack formation and delamination after actuation even without MEM incubation.

The covalent immobilization of PMNFs onto the 1 C actuator had little effect on the k, which was 0.24 N m^{-1} after immobilization, compared to 0.25 N m^{-1} without the immobilization. This could be explained by the fact that the PMNFs are not forming a solid layer but can be regarded as large individual biomolecules. However, after MEM incubation, the PMNF-induced mineralization significantly increased the k of the actuator with PMNFs to 0.34 N m^{-1}, which is more than 1.4-fold bigger than that before incubation. This clearly indicates the formation of the stiff mineral layer on top of the PPy, which causes the actuator to stop moving during the first cycle (Figure 4c), similar to our previous actuators that form bone.[17]

2.4. Mechanism of Delamination

The delamination processes seen in Figure S2, Supporting Information, and Figure 4b can be explained by the actuation mechanism. During the actuation process, that is, when applying the reduction/oxidation potential, the actuation force is generated by the expansion/contraction of the PPy film via the injection/ejection of ions and water solvent. This causes a stress distribution in the actuator, which results in the bending of the actuator (**Figure 9**a).[26,33] It is also important to note that

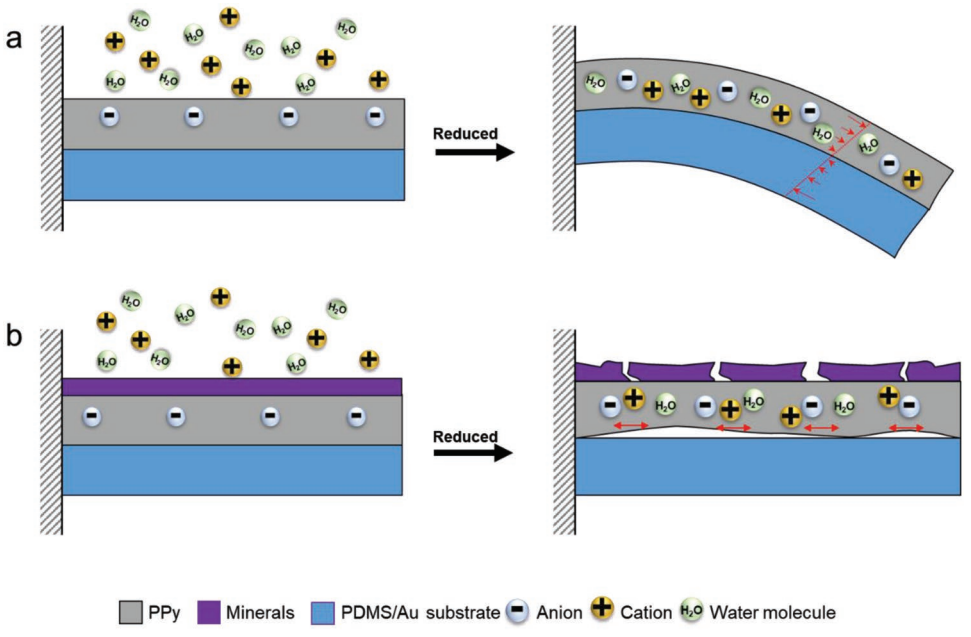

Figure 9. The schematic of the behavior of the actuator with PMNFs a) before mineralization and b) after mineralization. Before incubation, the volume change of PPy causes internal stress, as indicated by the arrows, which causes the PPy to bend. After the incubation, the bending is restricted due to the rigid mineral layer and layers delaminated and the mineral layer shows cracks.

the PPy layer is only physically attached to the PDMS/Au substrate and that the force exerted by the PPy scales with its thickness.[34] In the case of the 1 and 2 C actuators, the PPy exerted sufficient force to bend the actuator while at the same time the stress gradient at the PPy-Au/PDMS interface was not high enough to cause delamination. However, for the 3 C actuator, the stress gradient at the interface was too high and PPy delaminated, as seen in previous reports.[26,35]

As mentioned, in the actuator with PMNFs before MEM incubation, the PPy layer expanded due to the injection of cations and water during reduction, but the swelling force did not cause delamination. However, after MEM incubation, the same actuator showed an interesting phenomenon. After the initial stopping of the actuator in the first cycle, it started delaminating and cracking, that is, the grown mineral layer changed the mechanics of the actuator. The PPy near the mineral cannot expand since it is covalently attached to the stiff mineral layer, therefore, the generated stress gradient is now the highest at the PPy- PDMS/Au interface (Figure 9b). This now forms the weakest spot, and the actuator delaminates. Simultaneously, further PPy expansion causes even cracking of the thin and brittle mineral layer. This is different from our previous biohybrid actuators, where the mineral layer is grown in a 3D matrix of Alg gel, and is, therefore, markedly thicker, while the Alg gel functions similarly to the collagen in bone, giving the mineral layer more strength (flexibility and resilience).[17]

2.5. Improvement in the Adhesion of the PPy Layer on PDMS/Au Passive Substrate

To counteract the PPy cracking and delamination, a second Au layer with a rough texture was electrochemically plated on the Au layer to enhance the adhesion of PPy to Au, following the strategy of Bohn et al.[36] and Cui et al.[37] (Figure S8, Supporting Information). Next, these actuators with enhanced PPy-Au adhesion (addressed as EA-actuators) and with covalently attached PMNFs were actuated both before and after MEM incubation (**Figure 10**a,b). As can be seen, there no longer appeared cracks or delamination, indicating that the PPy film was indeed tightly attached to the EA gold layer. The actuator's displacement after MEM incubation (1 mm) decreased as compared to that before incubation (2 mm), while showing a normal cyclic actuation and stable currents (Figure 10c,d). In contrast to the Alg gel actuators,[17] the mineralization of PMNF by incubation in MEM was not sufficient to completely stop the actuator's movement (Figure 10c), due to the thin layer of the minerals, but it still led to a decrease of the displacement to half of that seen before incubation in MEM.

2.6. Immobilization of PMNFs in Gel Layer to Form 3D Minerals

Finally, to investigate whether indeed a thick and 3D structured bone layer results in a full stop of the actuator's movement,

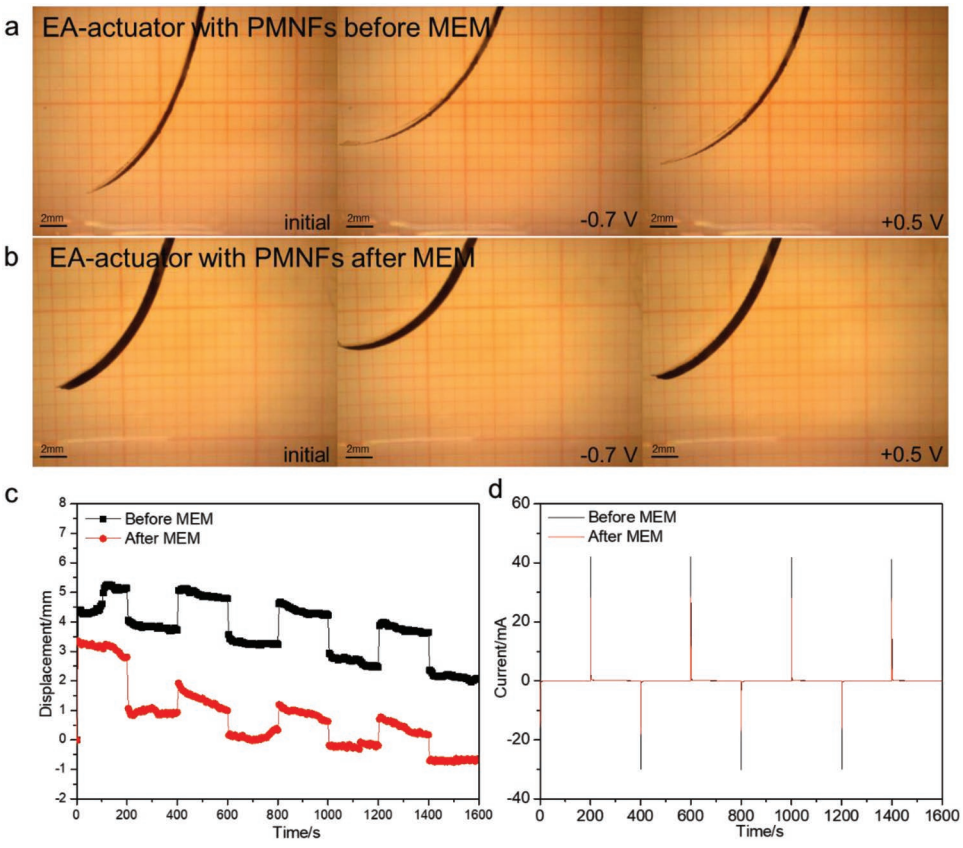

Figure 10. Actuation of EA-actuator with PMNFs a) before and b) after MEM incubation at initial reduction (–0.7 V) and oxidation (0.5 V) states. Corresponding c) displacement and d) current curves during the actuation. Reproduced with permission.[21] Copyright 2022, IEEE.

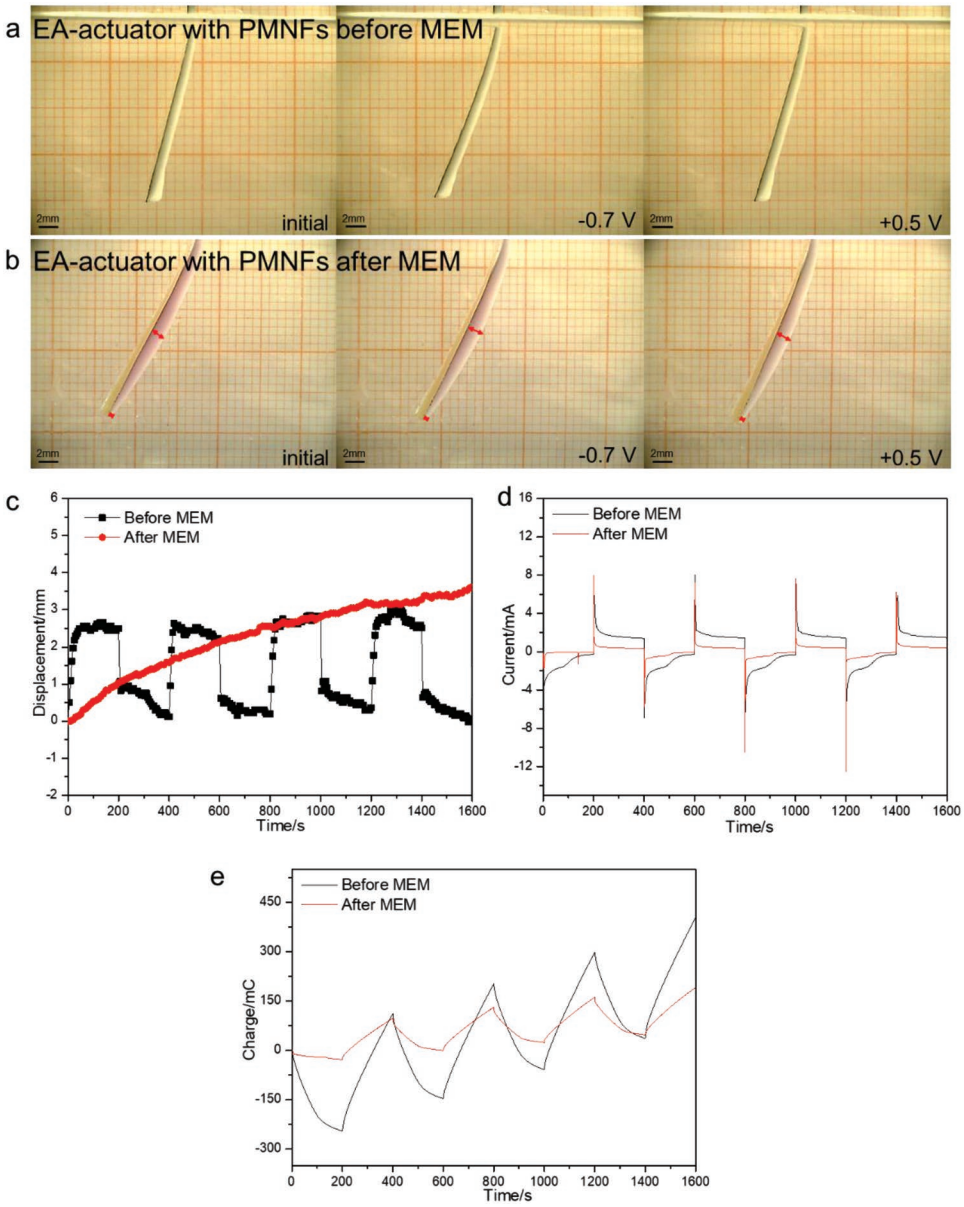

Figure 11. Actuation of EA-actuators with PMNFs a) before and b) after MEM incubation at initial reduction (–0.7 V) and oxidation (+0.5 V) states. Corresponding c) displacement, d) current curves, and e) charge during the actuation.

we fabricated an actuator with an Alg gel layer following the method reported previously.[17]

A PMNF-Alg gel layer was deposited on the PPy/(PSA) layer of the actuator, resulting in an EA-gel actuator with PMNFs. As shown in **Figure 11**, the Alg gel remained adhered to the PPy layer even after actuation, both before and after incubation. Moreover, while the displacement before incubation was about 3 mm, after MEM incubation, the PMNF-induced mineralization stiffened the Alg gel layer, indeed arresting the actuation during the initial two cycles. From the third cycle onward, a small 0.5 mm displacement was observed at the tip of the actuator only, while the central region of the actuator remained fixed. This is because the Alg layer at the tip was thinner than in the central part, leading to less formation of minerals, hence less bending stiffness at the tip, as shown by the red marks in Figure 11b.

Moreover, the current (Figure 11d) and charge (Figure 11e) of the actuators incubated in MEM were slightly decreased in the first two cycles, suggesting that the mineralization reduced the mechanical force of the actuator, while from the third cycle onward, they increased because the tip of the actuator started to move. Therefore, the performance of the EA-gel actuator with PMNFs confirmed that a thick mineralized layer is needed to completely stop the actuator's movement. In addition, the use of the gel matrix gives the mineral layer more strength.

3. Conclusion

We used a simple method to obtain a soft and mechanically robust PDMS/Au passive substrate by transferring SU 8 spin-coated pre-treated Au thin films from a silicon wafer to PDMS. Then, PPy doped with PSA was electropolymerized on the PDMS/Au passive substrate to obtain a PPy actuator. The functionalized PPy actuator was fabricated by immobilizing PMNFs on the PPy surface using the EDC/NHS covalent technique. This resulted in a variable stiffness actuator that could change from soft to stiff after PMNF mineralization. However, the PPy layer delaminated from the PDMS/Au due to the increased stiffness resulting from the PMNF mineralization. Therefore, we electroplated a second Au layer with a rough texture to improve the adhesion of the mineralized PPy-PMNF layer on PDMS/Au. However, since only a thin mineral layer was formed under covalent immobilization, the displacement of the EA-actuators with PMNFs could not be completely stopped after incubation. Indeed, when a 3D Alg gel functionalized with PMNFs on PPy was used instead of the direct immobilization of PMNFs on PPy, the stiffness of the mineralized layer was enhanced resulting in a full stop of the actuator, confirming that a thick mineralized layer could completely suppress the actuator's movement. In addition, the use of the gel matrix gives the minerals layer more strength, similar to collagen in natural bone. In this work, we have demonstrated two approaches to immobilize PMNFs on conducting polymers: one is using covalent (chemical) immobilization on the conducting polymer surface and the other is entrapping the PMNFs in a gel matrix. These two approaches provide more flexibility to immobilize PMNFs, or other biomolecules, for designing biohybrid variable stiffness actuators with different mechanical properties of the stiff segments. This gives new opportunities to choose the preferred method best suited for the application in mind. Designing variable stiffness actuators based on the self-creation of bone is complex and comprises many factors such as bone thickness and actuator geometry. Here, we have shown one aspect of how these factors interact and may give guidelines for the future design of such self-creating-bone actuators. These self-creating-bone actuators show a soft-to-hard phase change, which has many interesting applications. For instance, since they are soft and flexible at their initial state, devices comprising this phase change material could be tightly folded, wrapped, or packed and be inserted through a narrow orifice (needle, catheter), and thereafter, unfold and reshape or morph to their programmed final structure and induce to become rigid and build up their load-bearing structures (e.g., bone-like structure). In addition, this phase change process could be used in "4D printing or 4D manufacturing,"[6,38] where a device is first printed/manufactured and thereafter morphs into a more complex shape. The biohybrid materials as presented here need no special or complex chemistry reaction nor any special or potentially harmful conditions, for example, elevated temperature, high voltage, or UV light to achieve the soft-to-rigid phase change. Very mild conditions can be used: incubation at room temperature in a Ca^{2+} and phosphate-containing solution, such as the cell culture medium. Therefore, the PMNF-based actuator could be developed into variable-stiffness devices and used as a potential tool for tissue engineering, such as adhering to the bone to support or repair bone fractures. Additionally, this biohybrid material may potentially be applied to replace soft-hard interfaces, such as artificial tendons, that is, on one side the minerals can grow and adhere to bone, while the other side of the substrate side remains soft (e.g., PDMS or a gel).

4. Experimental Section

Materials: Pyrrole (Py) monomer (Fluka, Switzerland) was vacuum distilled prior to use and stored at −20 °C. Poly (4-styrenesulfonic acid-co-maleic acid) sodium salt (PSA, average Mw ≈20 000), sodium chloride (NaCl), MEM, sodium alginate (Alg), and ethanol were purchased from Sigma-Aldrich (St. Louis, MO, USA). Negative photoresist SU 8 3035 was acquired from Microchem (Ulm, Germany). Mr-Dev 600 developer was purchased from Micro Resist Technology (Berlin, Germany). PDMS elastomer kit (Sylgard 184) was obtained from Dow Corning (Midland, MI, USA). Gold-plating solution of $Na_3Au(SO_3)_2$ was obtained from Technic Inc. Amine coupling kit with EDC and NHS was purchased from Cytiva (Marlborough, MA, USA). Deionized water (DI, 18.2 MΩ) was obtained from Milli-Q Plus water equipment and used throughout the experiments.

PMNFs were isolated from pre-chondrogenic ATDC5 cells as previously reported.[18,19] Briefly, a total of 1×10^7 cells were collected in 1.5 mL tubes and resuspended in 1 mL of DI water. The cells were then ultrasonicated for 3 min for cell fragmentation, followed by a series of centrifugation steps ($800 \times g$ for 5 min, $1000 \times g$ for 10 min, $20\,000 \times g$ for 30 min, and $150\,000 \times g$ for 60 min), as reported.[18,19,39] The resulting PMNF pellet was collected, resuspended in DI water, and submitted to quantitative analysis of protein concentration using bicinchoninic acid assay (BCA) assay (Takara Bio Inc., Shiga, Japan).

Mineralization of PMNFs was induced by incubating them in MEM for up to 3 days.

Fabrication of PDMS/Au Passive Substrate: The fabrication procedures of the PDMS/Au passive substrate are shown in Figure 1. In brief, a piece of silicon (20 mm × 18 mm) was precoated with 1000 Å Au films (Au/Si) using thermal evaporation. An epoxy resin (SU 8 3035) was spin-coated onto the Au surface (SU 8/Au/Si) at 500 rpm (acceleration 300 rpm s^{-1}) for 10 s and 3500 rpm (acceleration 300 rpm s^{-1}) for 30 s. The SU 8/Au/Si wafer was soft and hard baked on a hotplate at 95 °C for 5 min each. The SU 8/Au/Si wafer was then developed using Mr-Dev 600 for 4 min to remove the SU 8 layer. The obtained Au/Si wafer was washed by immersing it in isopropanol for 3 min and dried with nitrogen.

PDMS prepolymer was prepared by mixing the two components in a 10:1 base-to-crosslinker ratio and degassed in a vacuum desiccator. The PDMS prepolymer was then spin-coated on the Au/Si wafer (PDMS/Au/Si) at 500 rpm (acceleration 250 rpm s^{-1}) for 30 s. The PDMS/Au/Si assembly was cured in an oven at 90 °C for 60 min. After that, the PDMS/Au passive substrate was peeled off from the Si wafer.

Fabrication of PDMS/Au/PPy Actuator: PDMS/Au/PPy actuator was fabricated by electropolymerization of PPy onto the PDMS/Au passive substrate. Electrochemical studies were performed with a potentiostat (Iviumstat, Ivium Technologies, Eindhoven, the Netherlands) set with a classical three-electrodes electrochemical cell configuration. The PDMS/Au passive substrate was used as the working electrode, Ag/AgCl (3 M NaCl; model RE-5B from BASi) as the reference electrode, and a stainless steel mesh (30 mm × 70 mm) as the counter electrode. PPy was electropolymerized at 0.6 V in 0.1 M Py and 2 mg mL^{-1} PSA solution, wherein the PSA served as the supporting electrolyte and as the source of counterions to compensate for the positive charge of the PPy backbone. Electropolymerization of PPy on PDMS/Au passive substrate was set to terminate after total charges of 1, 2, or 3 C were consumed. The obtained corresponding actuators were denoted as 1 C actuator, 2 C actuator, and 3 C actuator, respectively.

Fabrication of Actuator with PMNFs: The PDMS/Au/PPy actuator surface was immobilized with PMNFs via covalent binding through EDC/NHS technique. In brief, PDMS/Au/PPy actuator surface

bearing carboxylic acid groups (PPy(PSA) layer) was activated by a mixture of 200 µL EDC (400 mM) and 200 µL (200 mM) NHS for 50 min. After the removal of excess EDC/NHS with water, the PPy(PSA) surface side was immersed in a 500 µL solution containing PMNFs (100 µg mL^{-1} in water) for 2 h at room temperature. The PMNF-immobilized PDMS/Au/PP actuator was then washed with water and dried at room temperature. The actuator was denoted as an actuator with PMNFs.

Preparation of EA-Actuator with PMNFs: To enhance the adhesion between Au and PPy, a second Au layer with a rough texture was deposited on the PDMS/Au passive substrate, using the electrochemically plating method as described in refs. [36,37]. The PDMS/Au film was placed into an electrochemical cell containing the gold-plating solution of $Na_3Au(SO_3)_2$, stainless steel mesh counter, and Ag/AgCl reference electrodes. The electrochemical gold plating was performed using –0.9 V potential for 5 min. This modified electrochemical gold plating PDMS/Au passive substrate was named as PDMS/Au/EA passive substrate. Thereafter, the same procedures described in sections Fabrication of PDMS/Au/PPy Actuator and Fabrication of Actuator with PMNFs were used for PPy polymerization and PMNF modification. The fabricated actuator was denoted as EA-actuator with PMNFs.

Preparation of EA-Gel Actuator with PMNFs: Actuators with Alg gel and PMNF were prepared as follows. An amount of 500 µL of 2.5% Alg gel with 100 µg mL^{-1} of PMNFs was dropped onto the PDMS/Au/EA (2.5 cm × 2 cm) passive substrate, which was then immersed into 1 M $CaCl_2$ for 20 s to crosslink the Alg gel, as previously reported.[17] The formed PDMS/Au/EA/Alg(PMNF) device was electropolymerized in a three-electrode cell, containing 0.1 M pyrrole and 2 mg mL^{-1} PSA electrolyte to polymerize a PPy layer until 1 C charge was consumed, to form the PDMS/Au/EA/PPy1C/Alg(PMNF) actuator, which was denoted as EA-gel actuator with PMNFs.

Actuation Measurement of Actuators: Electrochemical actuation measurements of the different actuators were performed using the same electrochemical setup as described in the section Fabrication of PDMS/Au/PPy Actuator. Actuator strips of 2 mm × 20 mm, cut from a bigger sample, were set as the working electrode, immersed in 0.1 M NaCl solution (the initial state), and submitted to a double step potential with a reduction potential of –0.7 V for 200 s (reduction state) followed by an oxidation potential of 0.5 V for 200 s (oxidation state). Four cycles of the double-step potential were conducted for each sample. During the actuation process, the movements of the actuators were recorded using a portable USB microscope camera (Edge, Dino-Lite) with 1 mm graph paper as the background. The displacement of the actuator tip was obtained from the recorded video using a bespoke-programmed MATLAB R2017b-based script. To evaluate the stiffen actuators, the PPy actuators without PMNFs, PPy actuators with PMNFs, EA-actuator with PMNFs, and EA-gel actuator with PMNFs were incubated in MEM for 3 days, followed by the same actuation measurements described above.

Characterization: SEM images were collected using a Leo1550 Gemini (Zeiss, Germany) or an S-4800 (Hitachi, Tokyo, Japan) scanning electron microscope. Elemental analysis was performed using EDX (Oxford Instruments, Oxfordshire, UK) with an electron acceleration voltage of 20 kV. The stiffness value k in Equation (3) was measured by placing the tip of the lever arm transducer using the lever arm transducer (Cambridge Technology Inc. Model 200B, USA) at the tip of the actuator to measure the different positions. The k value was calculated from the parameters (i.e. F, L, and δ) in Equations (1), (2), and (3). The parameters L and δ were recorded by a camera and calculated by MATLAB, F was the settled input force by the lever arm transducer.

Sheet resistance was measured using a four-point probe model RM3000 test unit (Jandel Engineering Ltd., Leighton Buzzard, UK).

Supporting Information

Supporting Information is available from the Wiley Online Library or from the author.

Acknowledgements

This work was supported by the Japanese Society of the Promotion of Science, JSPS, Bridge Fellowship program (BR170502), KAKENHI (JP20H04534), Japan Science and Technology Agency, JST, FOREST Program, Grant Number JPMJFR210X, Swedish Research Council (VR2014-3079), Promobilia Foundation (F17603), and China Scholarship Council (201808330454). This work was also supported by a bilateral joint research project grant by JSPS (JPJSBP 120209923) and STINT, the Swedish Foundation for International Cooperation in Research and Higher Education, (MG2019-8171). The authors wish to thank Prof Jonas Stålhand at LiU for the scientific discussions.

Conflict of Interest

The authors declare no conflict of interest.

Data Availability Statement

The data that support the findings of this study are available from the corresponding author upon reasonable request.

Keywords

actuators, bone, mineralization, plasma membrane nanofragments, polypyrrole, soft actuators, variable stiffness

Received: October 1, 2022
Revised: November 25, 2022
Published online:

[1] M. Cianchetti, C. Laschi, A. Menciassi, P. Dario, *Nat. Rev. Mater.* **2018**, *3*, 143.
[2] a) A. Villoslada, A. Flores, D. Copaci, D. Blanco, L. Moreno, *Rob. Auton. Syst.* **2015**, *73*, 91; b) P. Maeder-York, T. Clites, E. Boggs, R. Neff, P. Polygerinos, D. Holland, L. Stirling, K. Galloway, C. Wee, C. Walsh, *J. Med. Devices* **2014**, *8*, 020933.
[3] B. C. Mac Murray, X. An, S. S. Robinson, I. M. van Meerbeek, K. W. O'Brien, H. Zhao, R. F. Shepherd, *Adv. Mater.* **2015**, *27*, 6334.
[4] S. Bauer, S. Bauer-Gogonea, I. Graz, M. Kaltenbrunner, C. Keplinger, R. Schwödiauer, *Adv. Mater.* **2014**, *26*, 149.
[5] M. Calisti, M. Giorelli, G. Levy, B. Mazzolai, B. Hochner, C. Laschi, P. Dario, *Bioinspiration Biomimetics* **2011**, *6*, 036002.
[6] S. Naficy, R. Gately, R. GorkinIII, H. Xin, G. M. Spinks, *Macromol. Mater. Eng.* **2017**, *302*, 1600212.
[7] W. Xu, D. H. Gracias, *ACS Nano* **2019**, *13*, 4883.
[8] M. Tyagi, J. Pan, E. W. Jager, *Microsyst. Nanoeng.* **2019**, *5*, 44.
[9] J. Xu, S. Ye, J. Fu, *J. Mater. Chem. A* **2018**, *6*, 24291.
[10] S. Gharazi, B. C. Zarket, K. C. DeMella, S. R. Raghavan, *ACS Appl. Mater. Interfaces* **2018**, *10*, 34664.
[11] a) G. Alici, G. Spinks, N. N. Huynh, L. Sarmadi, R. Minato, *Bioinspiration Biomimetics* **2007**, *2*, S18; b) K. Kaneto, E. Jager, G. Alici, H. Okuzaki, *Electromechanically Active Polymers*, **2016**, pp. 385–411.
[12] E. Smela, O. Inganäs, I. Lundström, *Science* **1995**, *268*, 1735.
[13] Z. Xu, D.-W. Wei, R.-Y. Bao, Y. Wang, K. Ke, M.-B. Yang, W. Yang, *ACS Appl. Mater. Interfaces* **2022**, *14*, 22521.
[14] H. T. Lee, F. Seichepine, G. Z. Yang, *Adv. Funct. Mater.* **2020**, *30*, 2002510.
[15] A. Tonazzini, S. Mintchev, B. Schubert, B. Mazzolai, J. Shintake, D. Floreano, *Adv. Mater.* **2016**, *28*, 10142.

[16] Z. Chen, W. Lu, Y. Li, P. Liu, Y. Yang, L. Jiang, *ACS Appl. Mater. Interfaces* **2022**, *14*, 30007.
[17] D. Cao, J. G. Martinez, E. S. Hara, E. W. Jager, *Adv. Mater.* **2022**, *34*, 2107345.
[18] E. S. Hara, M. Okada, N. Nagaoka, T. Hattori, T. Kuboki, T. Nakano, T. Matsumoto, *ACS Biomater. Sci. Eng.* **2018**, *4*, 617.
[19] E. S. Hara, M. Okada, T. Kuboki, T. Nakano, T. Matsumoto, *J. Mater. Chem. B* **2018**, *6*, 6153.
[20] a) M. Christophersen, B. Shapiro, E. Smela, *Sens. Actuators, B* **2006**, *115*, 596; b) E. Jager, O. Inganäs, I. Lundström, *Adv. Mater.* **2001**, *13*, 76.
[21] D. Cao, J. G. Martinez, E. S. Hara, E. W. Jager, presented at *2022 Int. Conf. on Manipulation, Automation and Robotics at Small Scales (MARSS)*, IEEE, Piscataway, NJ **2022**.
[22] T. Sekitani, Y. Noguchi, K. Hata, T. Fukushima, T. Aida, T. Someya, *Science* **2008**, *321*, 1468.
[23] a) I. Byun, A. W. Coleman, B. Kim, *J. Micromech. Microeng.* **2013**, *23*, 085016; b) S. C. Mannsfeld, B. C. Tee, R. M. Stoltenberg, C. V. H. Chen, S. Barman, B. V. Muir, A. N. Sokolov, C. Reese, Z. Bao, *Nat. Mater.* **2010**, *9*, 859.
[24] O. Graudejus, P. Görrn, S. Wagner, *ACS Appl. Mater. Interfaces* **2010**, *2*, 1927.
[25] a) M. H. Lee, J. Y. Lin, T. W. Odom, *Angew. Chem.* **2010**, *122*, 3121; b) A. M. Bowen, R. G. Nuzzo, *Adv. Funct. Mater.* **2009**, *19*, 3243.
[26] D. Melling, J. G. Martinez, E. W. Jager, *Adv. Mater.* **2019**, *31*, 1808210.
[27] a) A. Khaldi, A. Maziz, G. Alici, G. M. Spinks, E. W. Jager, presented at *Electroactive Polymer Actuators and Devices (EAPAD)*, SPIE, Bellingham, WA **2015**, 2015; b) A. Khaldi, A. Maziz, G. Alici, G. M. Spinks, E. W. Jager, *Sens. Actuators, B* **2016**, *230*, 818.
[28] M. Tyagi, G. M. Spinks, E. W. Jager, *Soft Rob.* **2021**, *8*, 19.
[29] a) A. S. Liu, M. A. Oliveira, *J. Braz. Chem. Soc.* **2007**, *18*, 143; b) J. Baumgartner, J.-I. Jönsson, E. W. Jager, *J. Mater. Chem. B* **2018**, *6*, 4665.
[30] N. Lobontiu, E. Garcia, *Mechanics of Microelectromechanical Systems*, Springer Science & Business Media, Springer, New York **2004**.
[31] a) P. Du, X. Lin, X. Zhang, *Sens. Actuators, A* **2010**, *163*, 240; b) M. Benslimane, P. Gravesen, K. West, S. Skaarup, P. Sommer-Larsen, presented at *Smart Structures and Materials 1999: Electroactive Polymer Actuators and Devices*, SPIE, Bellingham, WA **1999**.
[32] a) G. Alici, *Sens. Actuators, B* **2009**, *141*, 284; b) A. Maziz, C. Plesse, C. Soyer, C. Chevrot, D. Teyssié, E. Cattan, F. Vidal, *Adv. Funct. Mater.* **2014**, *24*, 4851.
[33] Q. Pei, O. Inganäs, *J. Phys. Chem.* **1992**, *96*, 10507.
[34] a) E. Smela, M. Kallenbach, J. Holdenried, *J. Microelectromech. Syst.* **1999**, *8*, 373; b) B. Shapiro, E. Smela, *J. Intell. Mater. Syst. Struct.* **2007**, *18*, 181; c) E. Smela, *J. Micromech. Microeng.* **1999**, *9*, 1.
[35] K. Idla, O. Inganäs, M. Strandberg, *Electrochim. Acta* **2000**, *45*, 2121.
[36] C. C. Bohn, M. H. Pyo, E. Smela, J. Reynolds, A. B. Brennan, *Abstr. Pap. Am. Chem. Soc.* **2002**, *223*, D60.
[37] X. Cui, D. C. Martin, *Sens. Actuators, A* **2003**, *103*, 384.
[38] a) S. E. Bakarich, R. Gorkin III, M. I. H. Panhuis, G. M. Spinks, *Macromol. Rapid Commun.* **2015**, *36*, 1211; b) M. López-Valdeolivas, D. Liu, D. J. Broer, C. Sánchez-Somolinos, *Macromol. Rapid Commun.* **2018**, *39*, 1700710; c) Y. Mao, K. Yu, M. S. Isakov, J. Wu, M. L. Dunn, H. J. Qi, *Sci. Rep.* **2015**, *5*, 13616; d) M. Tyagi, G. M. Spinks, E. W. Jager, *Smart Mater. Struct.* **2020**, *29*, 085032.
[39] J. M. Suski, M. Lebiedzinska, A. Wojtala, J. Duszynski, C. Giorgi, P. Pinton, M. R. Wieckowski, *Nat. Protoc.* **2014**, *9*, 312.